

# Comparison of $^{35}\text{Cl}$ NQR Spectra between the Mixed Crystals $\text{K}_2\text{Sn}_{1-x}\text{Re}_x\text{Cl}_6$ and the $\text{Al}^{3+}$ Doped Crystals $\text{K}_2\text{SnCl}_6:\text{Al}^{3+}$ \*,†

Y. M. Seo, J. Pelzl<sup>a</sup>, and C. Dimitropoulos<sup>b</sup>

Department of Physics, Korea University, Seoul, 136-701, Korea

<sup>a</sup> Institut für Experimentalphysik 3, Ruhr Universität Bochum, Germany

<sup>b</sup> Institute de Physique Experimentale, EPF Lausanne, Switzerland

Z. Naturforsch. **53 a**, 552–558 (1998); received March 24, 1998

$^{35}\text{Cl}$  Nuclear Quadrupole Resonance (NQR) has provided a valuable tool for investigating the local structure in mixed crystals  $\text{K}_2\text{Sn}_{1-x}\text{Re}_x\text{Cl}_6$  and  $\text{Al}^{3+}$  doped crystals  $\text{K}_2\text{SnCl}_6:\text{Al}^{3+}$ . The measured NQR line shapes and relaxation times of both kinds of impurity containing crystals in the cubic phase of the host  $\text{K}_2\text{SnCl}_6$  show markedly different impurity effects; static impurity effects in  $\text{K}_2\text{Sn}_{1-x}\text{Re}_x\text{Cl}_6$  and dynamic effects in  $\text{K}_2\text{SnCl}_6:\text{Al}^{3+}$ . The  $^{35}\text{Cl}$  NQR spectra of  $\text{K}_2\text{SnCl}_6:\text{Al}^{3+}$  near the transition temperature ( $T_c$ ) indicate the presence of pretransition of the local structure in the high temperature cubic phase.

## I. Introduction

Potassium hexachlorostannate ( $\text{K}_2\text{SnCl}_6$ ) belongs to the family of antiferrofluorites  $\text{A}_2\text{BX}_6$ , where A, B, and X represent respectively alkali, transition metal ions and halogens (Fig. 1a). Many of these compounds exhibit magnetic and displacive structural phase transitions. The structural phase transitions in  $\text{A}_2\text{BX}_6$  are driven by the condensation of the rotary lattice mode, which changes to the thermally activated rotation of the  $\text{SnX}_6^{2-}$  octahedra, the hindered rotation, at high temperatures. Thus the hindered rotation seems to be also of particular importance for the crystal instabilities and consequently to the structural transitions in  $\text{A}_2\text{BX}_6$ .

$\text{K}_2\text{SnCl}_6$  undergoes two structural phase transitions at 262 and 256 K on decrease of the temperature with change of the crystal symmetry from face centered cubic at high temperatures to monoclinic at low temperatures through an orthorhombic intermediate phase (Figure 1b).

In order to obtain a comprehensive description of the dynamical instabilities of the lattice, optic, and X-ray or neutron scattering as well as nuclear resonance investigation of the  $\text{A}_2\text{BX}_6$  mixed crystals, where both starting materials belong to the same antiferrofluorite family, have been intensively carried out [1 - 5].

The concentration dependence of the transition temperature  $T_c(x)$  is well described by the relation

$$T_c(x) = T_c(0) \frac{1 + ax}{1 + bx}, \quad (1)$$

where  $a$  and  $b$  are fitting parameters based on a mean field description of random systems [4]. This relation has been confirmed by the NQR study on mixed  $\text{A}_2\text{BX}_6$  crystals (Figure 2).

On the other hand, for  $\text{Al}^{3+}$  doped crystals, where the parent crystals are not isostructural, a smooth fit of impurities is hardly expected due to the topological and chemical differences of the starting materials. In this case, the substitution of impurities would produce various kinds of defects in the crystal. Therefore the NQR spectra of these kinds of impurity doped crystals would reflect the secondary impurity effect related to the static and dynamic properties of the impurity induced lattice defects.

In this contribution, the data on the variation of the  $^{35}\text{Cl}$  NQR spectra of the  $\text{K}_2\text{SnCl}_6$  matrix in mixed crystals  $\text{K}_2\text{Sn}_{1-x}\text{Re}_x\text{Cl}_6$  with  $\text{Re}^{4+}$  concentration are presented in the first part of Sect. IV, and the effect

\* Presented at the XIVth International Symposium on Nuclear Quadrupole Interactions, Pisa, Italy, July 20–25, 1997.

† A part of this work is based on the Ph. D. thesis submitted by Y. M. Seo to the Department of Physics, Ruhr Universität Bochum, Germany.

Reprint requests to Dr. J. Pelzl.



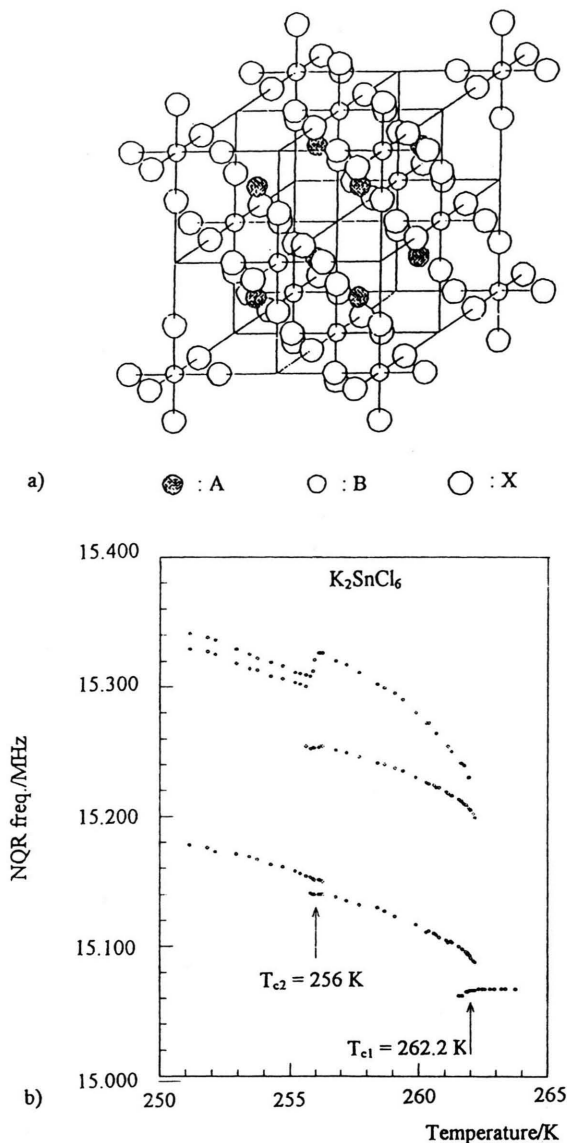


Fig. 1. a) Cubic antiferroite structure  $\text{A}_2\text{BX}_6$ ; b)  $^{35}\text{Cl}$  NQR frequency of  $\text{K}_2\text{SnCl}_6$  as a function of temperature near the transition temperatures  $T_{c1}$  and  $T_{c2}$ .

of the substitution of  $\text{Al}^{3+}$  ions on the  $^{35}\text{Cl}$  NQR of  $\text{K}_2\text{SnCl}_6$  in the  $\text{Al}^{3+}$  doped  $\text{K}_2\text{SnCl}_6$ ,  $\text{K}_2\text{SnCl}_6:\text{Al}^{3+}$  in the second part of Sect. IV. The  $^{35}\text{Cl}$  NQR spectra of  $\text{K}_2\text{Sn}_{1-x}\text{Re}_x\text{Cl}_6$  and  $\text{K}_2\text{SnCl}_6:\text{Al}^{3+}$  differ much. The NQR spectra of  $\text{K}_2\text{Sn}_{1-x}\text{Re}_x\text{Cl}_6$  reveal predominantly quasi-static impurity effects, while those of  $\text{K}_2\text{SnCl}_6:\text{Al}^{3+}$  indicate in many respects dynamic disorder, especially near  $T_c$ .

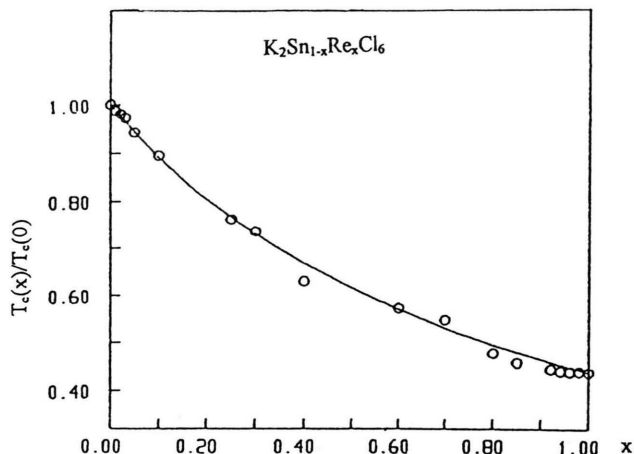


Fig. 2. Phase transition temperature of the mixed crystal system  $\text{K}_2\text{Sn}_{1-x}\text{Re}_x\text{Cl}_6$  as a function of impurity concentration. The solid line is the fit of (1) to the data.

## II. $^{35}\text{Cl}$ NQR in the Cubic Phase of $\text{K}_2\text{SnCl}_6$

The theoretical background of NQR can be found in [6]. The NQR hamiltonian is given by

$$\hat{H}_q = \hat{I} \cdot \vec{\hat{Q}} \cdot \hat{I}, \quad (2)$$

where  $\hat{I}$  is the nuclear spin operator and  $\vec{\hat{Q}}$  the quadrupolar tensor that contains the electric field gradient (efg) at the nuclear site and the quadrupole moment of the nucleus.

In the principal axes system, the quadrupole hamiltonian can be represented by two independent parameters, the maximum component of the efg  $V_{zz} = eq$ , where  $e$  is the electronic charge and  $\eta$  the asymmetry parameter, which is the measure of the deviation of the efg from the cylindrical symmetry along the  $z$  axis. In the case of  $^{35}\text{Cl}$ ,  $I = 3/2$ , the separation of the energy levels, which is doubly degenerate, yields a resonance frequency

$$\nu_q = \frac{e^2 q Q}{2h} \sqrt{1 + \frac{\eta^2}{3}}. \quad (3)$$

In the high temperature cubic phase of  $\text{K}_2\text{SnCl}_6$ , all chlorine nuclear sites are equivalent, and  $\eta = 0$  due to the cubic site symmetry, yielding one resonance frequency

$$\nu_q = \frac{e^2 q Q}{2h}. \quad (4)$$

### III. Sample Preparation and Experiment

$\text{K}_2\text{SnCl}_6$  and  $\text{K}_2\text{ReCl}_6$  were made by the methods described in [4]. Powdered samples of the mixed hexachlorometallates  $\text{K}_2\text{Sn}_{1-x}\text{Re}_x\text{Cl}_6$  were obtained by rapidly recrystallizing a highly saturated solution of  $\text{K}_2\text{SnCl}_6$  and potassium hexachlororhennate ( $\text{K}_2\text{ReCl}_6$ ) for  $0 \leq x \leq 1$ . Doping of  $\text{Al}^{3+}$  in  $\text{K}_2\text{SnCl}_6$  was achieved by evaporating a solution of  $\text{K}_2\text{SnCl}_6$  and aluminum chloride ( $\text{AlCl}_3$ ). From the results of atomic and spectroscopic analyses, the actual  $\text{Al}^{3+}$  concentration,  $x$ , in the  $\text{Al}^{3+}$  doped  $\text{K}_2\text{SnCl}_6$  crystals,  $\text{K}_2\text{SnCl}_6:\text{Al}^{3+}$ , is supposed to be much smaller than the nominal concentration over the whole range of  $x$  investigated, while in the mixed system the nominal concentration is generally in good agreement with the actual concentration. The homogeneity of the samples was checked by Raman scattering and X-ray diffraction analysis.

The NQR experiments were carried out with a Bruker pulsed spectrometer using a pulse width of around  $7 \mu\text{s}$  for the  $90^\circ$  pulse at the spectrometer frequency of 15 MHz. The temperature was regulated with a temperature controller (Cryogenic S 3010) by controlling the flow of liquid nitrogen drops and the heat current.

### IV. $^{35}\text{Cl}$ NQR Results and Discussion

#### 1. Mixed Crystals $\text{K}_2\text{Sn}_{1-x}\text{Re}_x\text{Cl}_6$

#### NQR Results at Temperatures Far Above the Transition Temperature

Besides the static line broadening, one important impurity ( $\text{Re}^{4+}$ ) effect on the resonance line of the  $\text{K}_2\text{SnCl}_6$  matrix is the appearance of the satellite lines in addition to the original resonance line (Figure 3). Two important features of the line spectra containing the original and satellite lines are as follows

a) The frequencies of the satellite lines are higher than that of the original line, and they are located regularly from the original resonance line with an equidistant sequence of OL - 1SL - 2SL - 3SL - 4SL, where OL denotes the original line and nSL the  $n$ -th satellite line.

b) The intensities of the original line and the satellite lines change systematically such that the relative intensity of the  $n$ -th line is described by the binomial function

$$I_n(x) = \frac{4!}{(4-n)!n!} (1-x)^{4-n} x^n, \quad (5)$$

where  $I_0(x)$  and  $I_n(x)$  are the intensity of the original line and the  $n$ -th satellite line, respectively.

Closer examination of the local charge distribution around the Cl site, which possesses fourfold symmetry about the Sn-Cl bonding axis, suggests that the satellite lines are produced if any of the 4 next nearest  $\text{Sn}^{4+}$  sites, from the position of the Cl nucleus under consideration, are occupied by  $\text{Re}^{4+}$  impurities. Therefore the intensity of the original and the satellite lines would be directly dependent on the probability for these lattice sites to be occupied by  $\text{Re}^{4+}$ . Figure 3 shows that the intensities predicted by (5) are in good agreement with the observed results. Here the frequency distance between neighbouring lines corresponds to the change in the value of  $q$  caused by each replacement of  $\text{Sn}^{4+}$  by  $\text{Re}^{4+}$ .

#### NQR Spectra Near the Structural Phase Transitions

With decreasing temperature both starting compounds  $\text{K}_2\text{SnCl}_6$  and  $\text{K}_2\text{ReCl}_6$  undergo the first structural phase transitions at 262 K and 111 K, respectively. A simple way to monitor the transition in  $\text{K}_2\text{SnCl}_6$  is observing the cubic line, which disappears suddenly at the transition temperature. Below  $T_c$  ( $= T_{c1}$  in Fig. 1b) three lines appear in  $\text{K}_2\text{SnCl}_6$ , corresponding to the orthorhombic structure. The general features of phase transitions in mixed crystals are as follows;

a) A monotonous shift of the transition temperature as a function of  $x$  between two transition temperatures of parent crystals  $T_c(0)$  for  $\text{K}_2\text{SnCl}_6$  and  $T_c(1)$  for  $\text{K}_2\text{ReCl}_6$  as predicted by (1) (Fig. 2) and

b) Rounding of the sharp anomalies at  $T_c$  (Fig. 4b) and a strongly nonexponential character in the spin-lattice relaxation near  $T_c$  (Figure 5a).

Smearing of the phase transition and the nonexponential relaxation can be easily understood in terms of the spatially macroscopic inhomogeneity in the impurity concentration in mixed crystals by considering (1) and the fact that, in most cases, the relaxation changes rapidly near the transition point. The nearly exponential decay of the spin magnetization recovery at temperatures far above  $T_c$  becomes increasingly nonexponential as the temperature approaches  $T_c$ , due to the inhomogeneous distribution of the impurities. Near  $T_c$ , the recovery curve is described actually

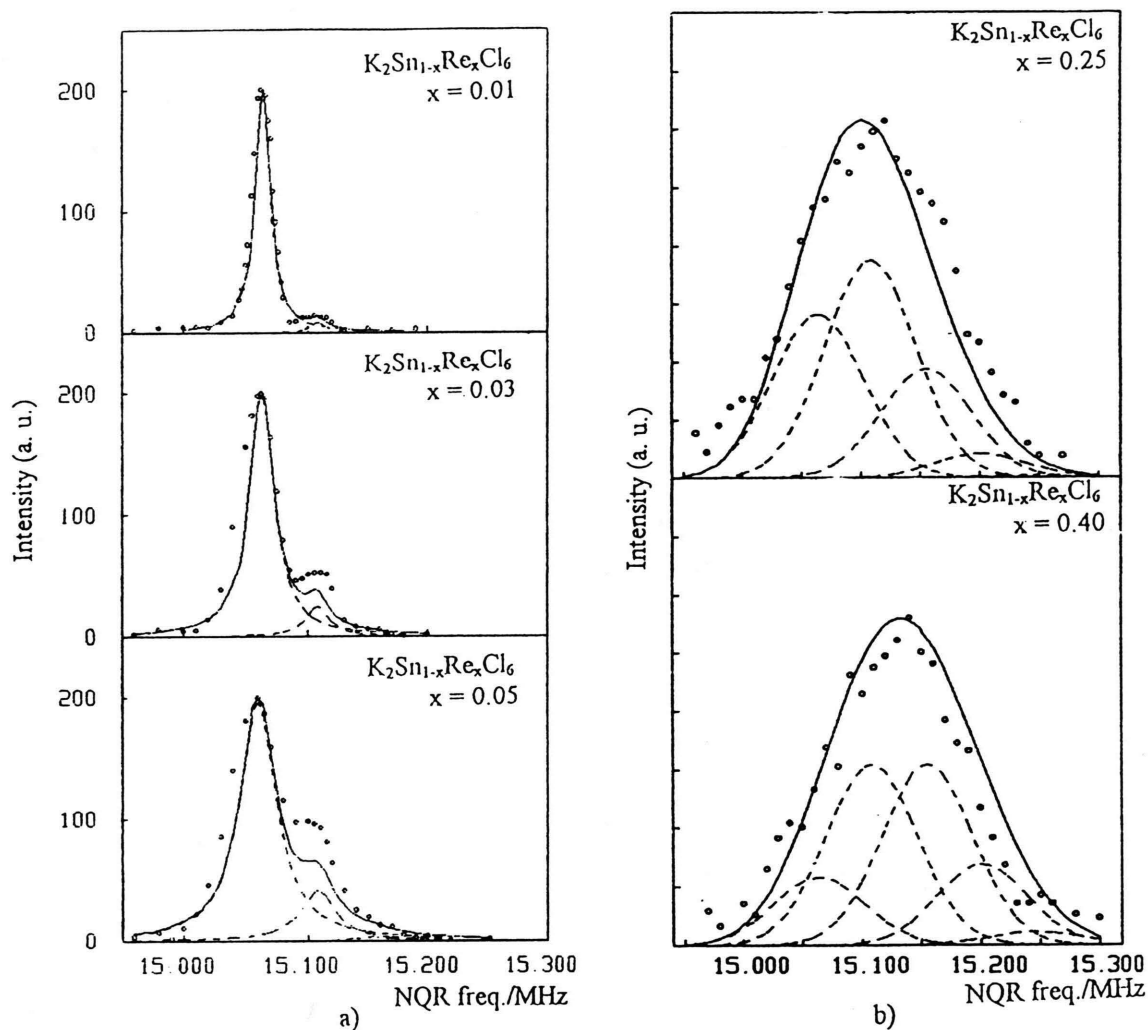


Fig. 3.  $^{35}\text{Cl}$  NQR line spectra of the  $\text{K}_2\text{SnCl}_6$  structure in  $\text{K}_2\text{Sn}_{1-x}\text{Re}_x\text{Cl}_6$  for a) small  $x (\leq 0.05)$  and b) large  $x (0.25 \leq x \leq 0.40)$ . The dashed lines denote the individual line (original and satellite lines) intensities, and the solid line the sum of all line intensities.

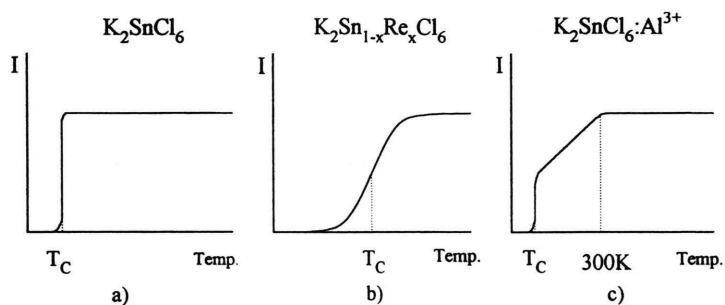


Fig. 4. Schematic representation of the cubic line intensity around the transition temperature for a)  $\text{K}_2\text{SnCl}_6$  ( $T_c = 262 \text{ K}$ ), b)  $\text{K}_2\text{Sn}_{1-x}\text{Re}_x\text{Cl}_6$ , and c)  $\text{K}_2\text{SnCl}_6:\text{Al}^{3+}$  ( $T_c = 262 \text{ K}$ ).

by a large number of exponential functions, each of which is represented by its own spin-lattice time  $T_1$  (Figure 5a). The strongly nonexponential character of the recovery curve near  $T_c$  is again a sign of the

macroscopic spatial inhomogeneities in the impurity concentration in mixed crystals.

Both phenomena, the appearance of the satellite lines and the strongly nonexponential spin lattice

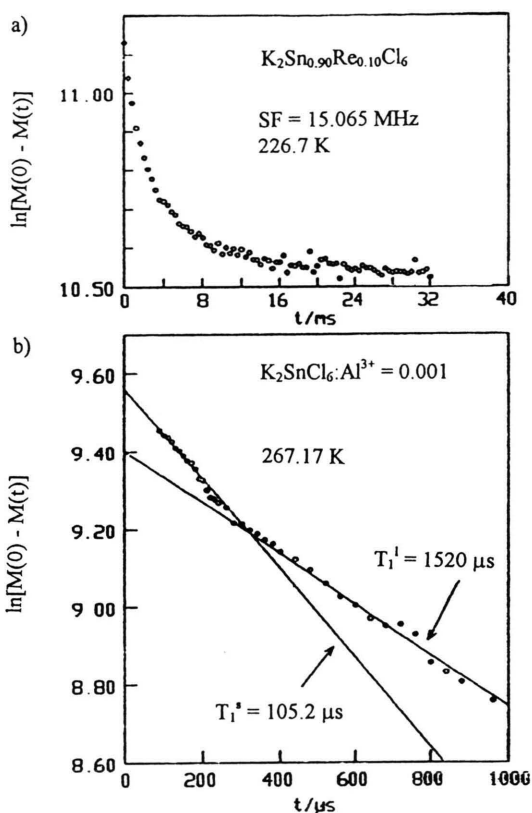


Fig. 5. Typical recovery of the chlorine nuclear magnetization in a)  $\text{K}_2\text{Sn}_{1-x}\text{Re}_x\text{Cl}_6$ , and b)  $\text{K}_2\text{SnCl}_6:\text{Al}^{3+}$ .

relaxation near  $T_c$  indicate that in the mixed crystals the dominant impurity effect on the  $^{35}\text{Cl}$  NQR is a static effect caused by the static random distribution of  $\text{Re}^{4+}$  ions at the  $\text{Sn}^{4+}$  sites and the spatially inhomogeneous distribution of the  $\text{Re}^{4+}$  concentration.

## 2. $\text{K}_2\text{SnCl}_6:\text{Al}^{3+}$

The NQR spectra of  $\text{K}_2\text{SnCl}_6:\text{Al}^{3+}$  contrast sharply to those of the mixed crystals  $\text{K}_2\text{Sn}_{1-x}\text{Re}_x\text{Cl}_6$  due to the crystallographic and chemical differences between the starting materials.

### NQR Frequency and Line Width

Figure 6 displays the line width of  $\text{K}_2\text{SnCl}_6:\text{Al}^{3+}$  as a function of the logarithmic impurity concentration (solid line). The concentration dependence of the line width of the mixed system is also shown for comparison (dashed line).

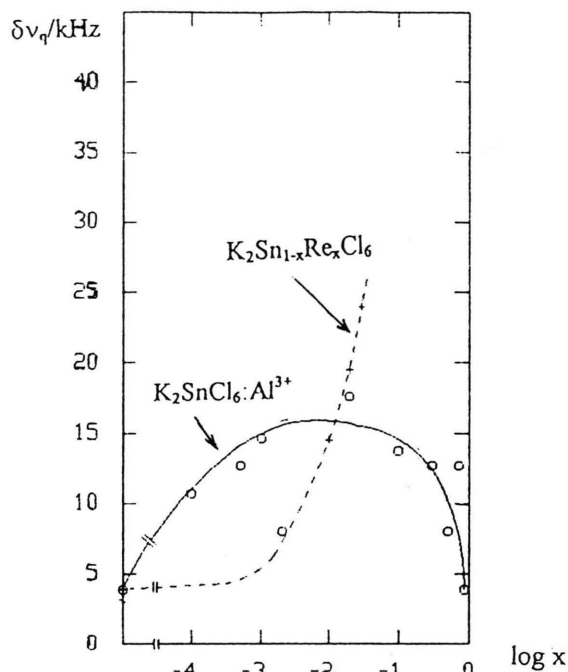


Fig. 6. Plot of the line width  $\delta\nu_q$  against  $\log x$ . The solid line and dashed line are guides to the eye. o :  $\text{K}_2\text{SnCl}_6:\text{Al}^{3+}$ ; + : mixed crystals.

The line width of the doped crystal over the impurity content investigated ( $0 \leq x \leq 0.85$ : nominal concentration) is restricted at room temperature to the values of 3.9 ~ 17 kHz, whereas in the mixed system the maximum value of the line width amounts to ~ 100 kHz (Figure 3b). The dependence on the impurity concentration of the line width is peculiar compared to that of  $\text{K}_2\text{Sn}_{1-x}\text{Re}_x\text{Cl}_6$ . The line width increases at first with increasing  $\text{Al}^{3+}$  concentration till it approaches a maximum value of ~ 17 kHz at about  $x = 0.02$ . Above this concentration, the line width decreases again with further increase of  $x$  and reaches finally the value at  $x = 0.85$ , which is essentially the same as that of the pure  $\text{K}_2\text{SnCl}_6$ . This line width behaviour differs much from that of the mixed crystal system  $\text{K}_2\text{Sn}_{1-x}\text{Re}_x\text{Cl}_6$ , where the line width seems to be relatively insensitive against impurity below  $x = 0.01$ , and above this concentration it diverges abruptly with increasing  $x$  (Fig. 6: +, dashed line).

The fact that the line width increases by no more than ~ 17 kHz with further increase in impurity content implies that there is a line narrowing because of the fast motion of lattice defects. The concentration dependence of the line width indicates that, at small concentration, immobile defects are produced



predominantly and these defects contribute to the line broadening resulting in a rapid increase in line width with increasing concentration. With further increase in concentration the fraction producing mobile lattice defects becomes more and more predominant. Because of their fast motion, the line broadening is limited to the maximum value of 17 kHz, and it decreases even again with further increase in concentration  $x$  due to the increase in the density of the mobile lattice defects approaching again the value comparable to the line width of the pure  $\text{K}_2\text{SnCl}_6$ .

### Temperature Dependence of Relaxation

High temperatures in the cubic phase can be divided into two regions at around 300 K according to the temperature behaviour of the relaxation times. Above 300 K, the temperature dependence of the relaxation times  $T_1$  and  $T_2$  is essentially the same as that of the pure  $\text{K}_2\text{SnCl}_6$ . The main relaxation mechanism here is, for both  $T_1$  and  $T_2$ , the thermally activated hindered rotation of the  $\text{SnCl}_6^{2-}$  octahedra, whose relaxation times have an exponential temperature dependence.

Below 300 K, both the magnetization recovery for  $T_1$  and the spin echo decay for  $T_2$  become nonexponential. In fact, they can be represented exactly by two exponential functions corresponding to two kinds of relaxation times, the shorter (s) and the longer (l) time  $T_1^s, T_2^s$  and  $T_1^l, T_2^l$ , respectively (Figure 5b). This double exponential character becomes more and more pronounced as the temperature approaches  $T_c$  from above (Figure 7). Though the presentation of the data on the spin echo decay for  $T_2$  are here omitted, they show also clearly the double exponential character, whose temperature dependence is exactly the same as that for  $T_1$ . By comparing with the relaxation time in the pure  $\text{K}_2\text{SnCl}_6$ , the longer relaxation time can be immediately identified to be of the same kind as that occurring in the pure  $\text{K}_2\text{SnCl}_6$ .

Double exponential magnetization recovery and spin echo decay curves corresponding to the longer and shorter relaxation times imply that the crystal consists of two sublattices, which are subject to the shorter and longer relaxation. The fact that the relaxations are represented here only by two exponential function, while the relaxation in the mixed crystals  $\text{K}_2\text{Sn}_{1-x}\text{Re}_x\text{Cl}_6$  near  $T_c$  contains a large number of exponential functions, suggests that the substitution of impurities here induces not a spatial inhomogeneity

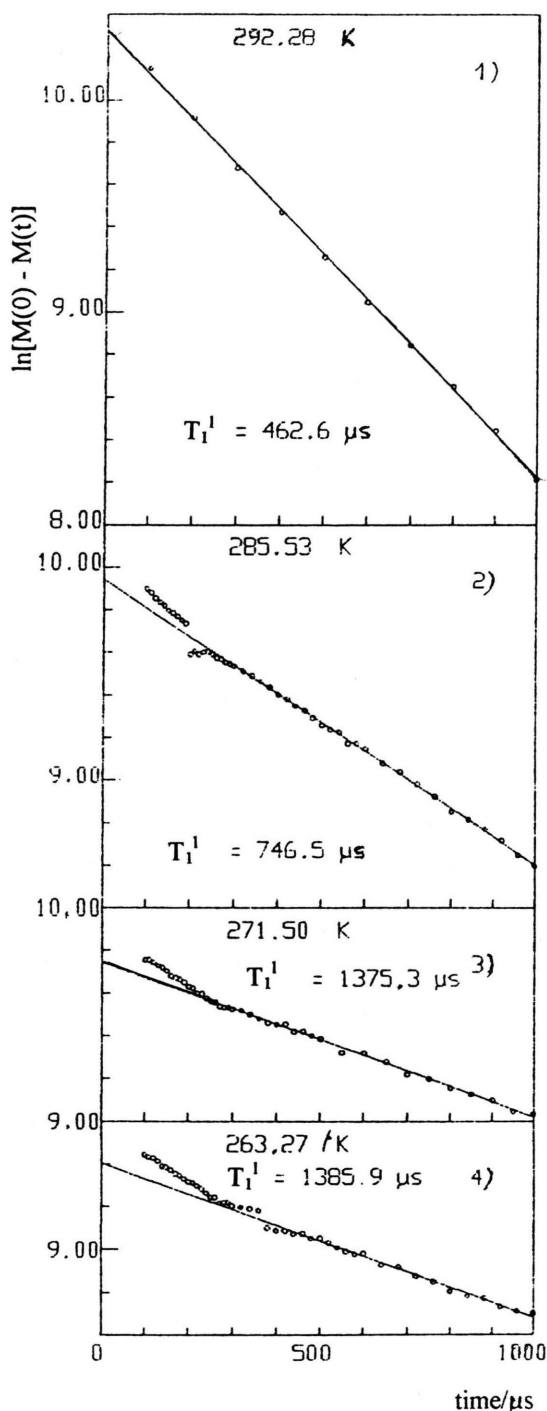


Fig. 7. A semi-logarithmic plot of the recovery of the  $^{35}\text{Cl}$  nuclear magnetization in  $\text{K}_2\text{SnCl}_6:\text{Al}^{3+}$ ,  $x = 0.0005$  in the cubic phase at temperatures near  $T_c$ .

but a dynamic inhomogeneity, i. e., two sets of sublattices which are different in lattice dynamics.

Temperature Behaviour of  $T_1^s$  and  $T_2^s$   
at  $T_c \leq T \leq 300\text{ K}$

The distinctive features of both short relaxation times  $T_1^s$  and  $T_2^s$  are as follows.

a) Both  $T_1^s$  and  $T_2^s$  values are roughly the same if they are measured at the same temperature.

b) The fraction of the shorter relaxation increases at the expense of that of the longer relaxation as the temperature approaches  $T_c$  (Figure 7).

The same values of  $T_1^s$  and  $T_2^s$  imply that the relaxation is nonresonant, i. e., it is not induced by the lattice vibrations but by the strong fluctuation of local fields.

On the other hand, the cubic line intensity shows an unusual temperature behaviour near  $T_c$  (Figure 4c); With decreasing temperature the line intensity begins to decrease at 300 K, just at which the shorter relaxation begins to appear. The line intensity decreases further till the temperature becomes  $T_c = 262\text{ K}$ , at which the rest of the line intensity drops sharply. This critical behaviour of the line intensity apparently differs from the rounding of the critical anomaly in mixed crystals caused by the static inhomogeneity in the crystal (Fig. 4b). Comparing with the temperature dependence of the shorter relaxation, it can be easily noticed that the temperature behaviour of the shorter relaxation is responsible for the unusual critical behaviour of the cubic line intensity near  $T_c$ .

All these features in  $\text{K}_2\text{SnCl}_6:\text{Al}^{3+}$  indicate the presence of a pretransition of local structures in the high temperature cubic phase, that execute a slow

structural fluctuation between the high temperature cubic phase and the low temperature phase.

A similar phenomenon was previously observed in the  $^{35}\text{Cl}$  NQR investigation of  $\text{K}_2\text{OsCl}_6$  by [7]. However the double exponential character was observed only for the spin-lattice relaxation corresponding to  $T_1^s$  and  $T_1^l$  in the powder sample. In their study an explanation for the presence of  $T_1^s$  was given in terms of the formation of dynamic clusters fluctuating between the high and low temperature phase.

## Summary

The mixed crystals  $\text{K}_2\text{Sn}_{1-x}\text{Re}_x\text{Cl}_6$  and the  $\text{Al}^{3+}$  doped  $\text{K}_2\text{SnCl}_6$  show quite different impurity effects on NQR spectra.

In  $\text{K}_2\text{Sn}_{1-x}\text{Re}_x\text{Cl}_6$ , the presence of satellite lines at room temperature and the strongly nonexponential recovery curve of the chlorine nuclear magnetization are attributed to the random distribution of  $\text{Re}^{4+}$  ions at the  $\text{Sn}^{4+}$  sites and the spatial inhomogeneity in the  $\text{Re}^{4+}$  concentration.

In  $\text{K}_2\text{SnCl}_6:\text{Al}^{3+}$ , the double exponential character of the recovery curve of the nuclear magnetization for  $T_1$  and the decay curve of the spin echo for  $T_2$  below 300 K indicate that the lattice consists of two sublattices, which are subjected to different lattice dynamics corresponding to the shorter relaxation times  $T_1^s$ ,  $T_2^s$  and the longer relaxation times  $T_1^l$ ,  $T_2^l$ .

The critical behaviour of the shorter relaxation times  $T_1^s$ ,  $T_2^s$  and their nonresonant character indicate the presence of pretransition local structures in the cubic phase, that fluctuate between the high temperature cubic phase and the low temperature phase.

- [1] Y. M. Seo, J. Pelzl, and C. Dimitropoulos, *Z. Naturforsch.* **41a**, 311 (1986).
- [2] J. Pelzl, V. Waschk, Y. M. Seo, and C. Dimitropoulos, *J. Mol. Str.* **11**, 363 (1983).
- [3] C. Dimitropoulos, J. Pelzl, H. Lerchner, M. Regelsberger, K. Roessler, and Al. Weiss, *J. Mag. Res.* **30**, 415 (1978).
- [4] V. Waschk, Ph. D. thesis Ruhr university Bochum, Germany (1982).
- [5] J. Pelzl, B. Arnscheidt, C. Dimitropoulos, and Y. M. Seo, *J. Korean Phys. Soc.*, to be published.
- [6] See, for example, T. P. Das and E. L. Hahn, *Nuclear Quadrupole Resonance Spectroscopy*, Solid State Physics, Suppl. 1, Academic Press, New York 1958; M. Bloom, E. L. Hahn, and B. Herzog, *Phys. Rev.* **97**, 6199 (1955).
- [7] C. A. Martin and R. L. Armstrong, *J. Mag. Res.* **20**, 411 (1975).